Journal of Applied Fluid Mechanics, Vol. 10, No. 6, pp. 1537-1546, 2017.
Available online at www.jafmonline.net, ISSN 1735-3572, EISSN 1735-3645.
DOI: 10.29252/jafm.73.245.27492

A Computational Study on the Performance Improvement of Low-Speed Axial Flow Fans with Microplates

D. Luo[1], D. Huang[1†], X. Sun[1], X. Chen[1] and Z. Zheng[2]

[1] *School of Energy and Power Engineering, University of Shanghai for Science and Technology, Shanghai 200093, China*
[2] *Aerospace Engineering Department, University of Kansas, Lawrence, KS, 66045-7621, USA*

†*Corresponding Author Email: dghuang@usst.edu.cn*

(Received December 13, 2016; accepted July 16, 2017)

ABSTRACT

This paper proposes the use of microplates as a new flow control device to suppress boundary layer separation on blades and thus improve the aerodynamic performance of a low-speed axial flow fan. A computational study is performed by means of computational fluid dynamics (CFD) simulations. Numerical investigations are carried out based on Reynolds-averaged Navier-Stokes (RANS) method. The shear stress transport (SST) turbulence model and high-quality computational grids are adopted for CFD simulations. An exhaustive comparison of the fans with and without control has been conducted in terms of characteristic curves, streamlines and pressure distributions. The purpose of this work is to better understand the underlying flow control mechanisms of microplates. It is found that the total efficiency is slightly lowered when the controlled fan operates at the design flow rate. However, as the flow rate changes, the total efficiency of the controlled fan varies more gently than the original fan without control. Traced streamlines show that flow separation on blade surfaces is effectively controlled and radial flow migration on the suction surface is evidently diminished. Numerical results indicate that microplates significantly alleviate fan stall and have considerable beneficial effects on fan performance.

Keywords: Axial flow fan; Flow control; Microplate; Computational fluid dynamics (CFD).

NOMENCLATURE

D_c	diameter of casing wall	x, y	circumferential and axial coordinates
D_h	diameter of hub	X, Y	circumferential and axial distances
H	height of microplate		
L	length of microplate	φ	flow coefficient
LE	leading edge	ψ	static pressure coefficient
P_s	static pressure	τ	torque of the rotor
P_t	total pressure	θ	setting angle of microplate
Q	volumetric flow rate	ω	angular velocity
TE	trailing edge	ρ	air density
u_a	average axial velocity	η	total efficiency
u_c	tangential blade-tip velocity	Δ	difference in the flow value between two reference surfaces
W	width of microplate		

1. INTRODUCTION

Fans have been widely used in many industrial applications such as dryers, cooling apparatuses, cabin air recirculation systems, etc. Low-speed axial flow fans, at a smaller scale, are commonly used for augmenting heat transfer particularly for cooling the electric or electronic devices. Flow separation and energy loss are inevitable in fans due to their complex three-dimensional geometries. Aerodynamic efficiency is one of the main factors to be considered in evaluating the fan performance.

Various flow control techniques are applied in fans to suppress flow separation and enhance their performance. These techniques are mainly classified as active or passive methods based on energy expenditure. Bianchi *et al.* (2013) gave an overview of control techniques for industrial fans.

Performance enhancement for axial flow fans has been investigated over several decades through various means. Air separator was proposed by Miyake *et al.* (1987) to improve the unstable characteristics of axial flow fans. The air separator bled a part of fluid near the blade tip and reintroduced it into the main-stream flow. This equipment was tested to be useful for fans even at a heavy rotating stall, whereas the efficiency of fans equipped with this device could be slightly reduced (Sheard *et al.* 2011, Corsini *et al.* 2014). Yamaguchi *et al.* (2010) designed radial-vaned air separators for an axial flow fan in their experiment and studied their stall suppression effects. Recess vaned casing treatment was applied by Azimian *et al.* (1990) and Hill *et al.* (1998) to axial flow fans to improve the stall margin and pressure rise. Blade-tip modifications were adopted by Corsini *et al.* (2009, 2010) to control the leakage vortex and reduce noise in axial flow fans. Other investigations of control techniques for fans and compressors can be found in the references (Corsini *et al.* 2013, Bianchi *et al.* 2012, Suder *et al.* 2001, Lemire *et al.* 2009). Although these techniques have the effect of stabilizing the performance of axial flow fans, the fan efficiency is typically reduced by 2~5 percent when the fans are under flow control, which is hard to agree with the increasing demands of efficiency enhancement.

This paper presents a new type of passive flow control device to stabilize the fan performance and meanwhile increase the fan efficiency. Microplates are adopted to be installed near the leading edges of blades and located close to the suction side. The purpose is to suppress flow separation on the suction surfaces when the fan operates in deep stall. The length of microplates is chosen to be 1/38 of the blade chord length at mid span. It is believed that such a small sized plate would not be severely detrimental to the fan peak efficiency. Computational fluid dynamics (CFD) analysis of the fans with and without control is then performed to confirm the validity of this proposed technique.

At present, CFD is one of the most important tools to design and analyze flow problems involved in turbomachinery (Pinto, *et al.* 2017). The design cycles and cost in turbomachinery can be significantly reduced with the aid of CFD. As a powerful tool, it is widely used to simulate the flow fields of rotating machinery such as fans and compressors. Zhu *et al.* (2005) carried out CFD investigations of the tip-region flows in an axial ventilation fan. Their numerical results are in generally good agreement with the experiment data. Kim *et al.* (2011, 2014) conducted optimizations for axial flow fans to enhance their aerodynamic performance, based on the Reynolds-averaged Navier-Stokes (RANS) method. The CFD simulations were performed using the commercial software ANSYS CFX and shear stress transport (SST) turbulence model (Menter 1994). CFX software and SST turbulence model were also adopted by Khaleghi (2015a, 2015b) to investigate the stall inception and control in a transonic fan. Louw *et al.* (2014) numerically investigated the flow fields in an axial flow fan at low flow rates. Radial flow around the fan blades was clearly demonstrated in their CFD simulations. Pogorelov *et al.* (2016a, 2016b) performed large eddy simulation (LES) for an axial fan focusing at the turbulent structures in the vicinity of tip-gaps. Vortex development near the blade tip was captured by their LES investigation.

The main objective of this investigation is to preliminarily assess the passive control effects of microplates on the fan performance through CFD simulations. Comparison between the characteristics of the fans with and without control was carried out. The detailed flow fields in the two fans were demonstrated to reveal the underlying flow control mechanisms.

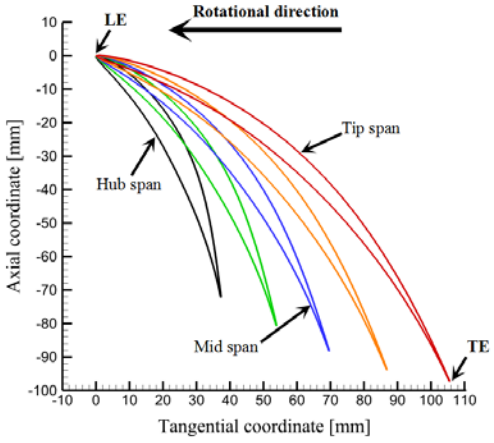

(a)

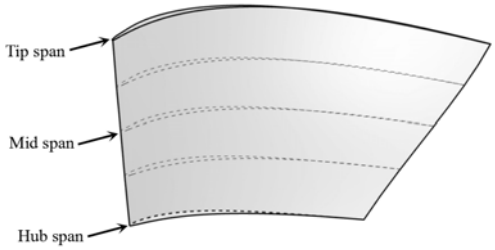

(b)

Fig. 1. Sections of blade profiles from hub to tip.

2. GEOMETRY DESCRIPTION

A small axial flow fan was used in the present investigation. The rotor comprises of eight twisted blades mounted on the inner hub and is shrouded with a design tip clearance of 2.5 mm. The chord length and stagger angle of the blades were changed with the span. Sections of blade profiles from hub to tip are shown in Fig. 1. The required static pressure rise is 45 Pa at a design volume flow rate

20 m^3/min. The fan is operated at a speed of 890 rpm, the casing and hub diameters are 300 mm and 165 mm respectively, and the hub-to-tip ratio is 0.56.

To improve the original fan performance, eight straight microplates were mounted on the inner hub and placed near the leading edges of the blades. The small axial flow fan equipped with microplates is shown schematically in Fig. 2. The microplates are featured by rounded-corners and their relative locations to the blades are shown in Fig. 3.

The circumferential and axial distances (X, Y) between the center of microplate and the leading edge of the fan blade are 0 and 3 mm, respectively. The setting angle of microplates chosen is θ=20° (measured from circumferential direction). The dimensions of each microplate in length L, width W and height H are 3 mm, 1.5 mm and 65 mm, respectively. The height of microplates chosen is the same as the height of blades, while the length, width and setting position of the microplate were optimized in the sense that the fan efficiency could be improved when the fan operates at off-design conditions, after much trial and error.

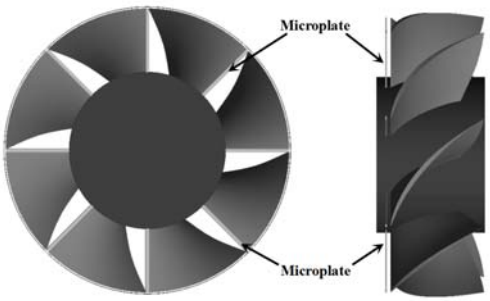

Fig. 2. Front and side views of the axial flow fan equipped with microplates.

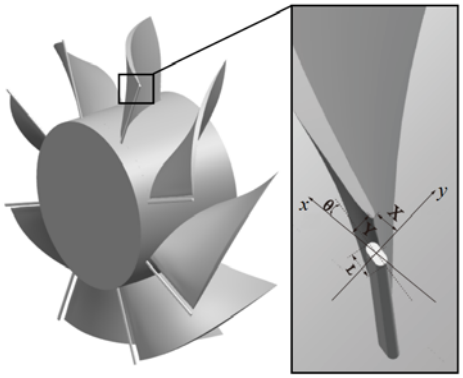

Fig. 3. Depiction of the relative locations of the microplate.

3. NUMERICAL METHODOLOGY

Blade profile creation was performed by Blade-Gen, and then the mesh was created using Pointwise software. All subsequent computational analyses were carried out using the commercial software ANSYS CFX 15.0. The three-dimensional incompressible RANS equations were discretized using the finite volume method. A high-resolution scheme with second-order spatial accuracy was adopted to solve the convection-diffusion equations. Steady simulation was performed and the *k-ω* based SST model (Menter 1994) was chosen as a turbulence closure.

The computational domain for the present numerical analysis includes dual passages of the axial flow fan, as shown in Fig. 4. The two blades and the inner hub surface are kept rotating at the design rotational speed, whereas the casing wall (not shown in Fig. 4) together with the inlet and outlet domains are considered to be static. The total pressure is fixed at the inlet domain, while the designed mass flow rate is set at the outlet. A quarter of the rotor flow domain is resolved to reduce the total computational cost. Therefore, periodic boundary conditions are applied at the two circumferential surfaces. All solid surfaces in the computational domain are treated as adiabatic and no-slip wall. Air at 25 °C is chosen as the working fluid. The same boundary conditions as above were specified in previous investigations (Kim *et al.* 2011, Kim *et al.* 2014).

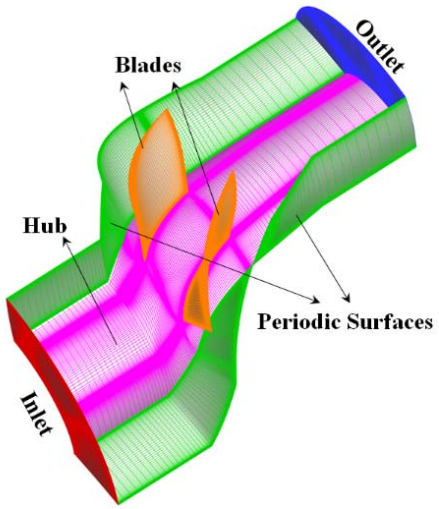

Fig. 4. Computational domain for the axial flow fan.

A hexahedral grid system was employed for the present study. The mesh is clustered toward all solid surfaces. Near-wall grid refinement was conducted to ensure the nondimensional wall distance $y^+<2$ for an accurate resolution of the wall shear stress. Additionally, 26 grid points were adopted to model the tip clearance along the span. Two different sets of structural grids were created for numerical analysis in this study. A total of approximately 4.26×10^6 and 6.19×10^6 grid cells were adopted for the coarse and fine grids, respectively. The grid distributions on the blade surfaces for the two grids are depicted in Fig. 5. O-type grids near the surfaces of both blades and

microplates were built to accurately resolve the boundary layers. H-type grids were used in other regions. The grid topology designed for the original fan without microplates is almost identical to that for the fan equipped with microplates, as shown in Fig. 6, in order to better evaluate the flow control effectiveness of microplates, after minimizing the effects of different grids on numerical resolutions. 41 wall-normal grid points are used in the gap between the fan blade and the microplate. The grid spacing growth rate is kept within 1.15 in the wall-normal direction.

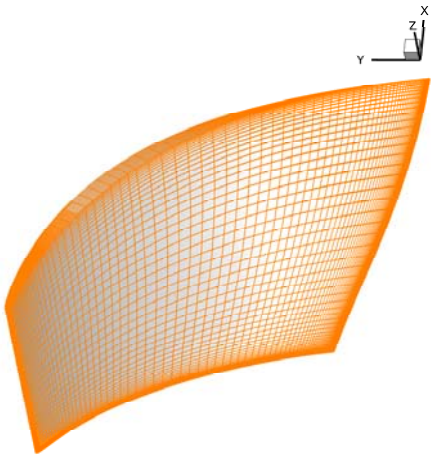

(a) Coarse grid

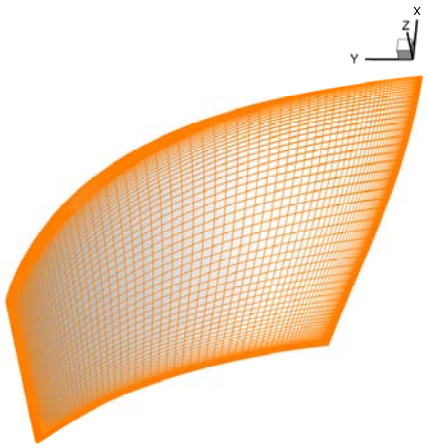

(b) Fine grid

Fig. 5. Blade surface grid.

The grid should have been constructed with simple blocks, if the microplates were not considered, and much coarser grid could have been adopted. When the microplates are introduced, such a complex grid topology is designed for both the original and controlled fans, in order to ensure that the same high-quality O-type grids are generated at the locations of microplates. In previous RANS investigations, the total number of grid points for one blade passage is mainly varied from 2.2×10^5 to 6.1×10^5 (Zhu *et al*., 2005; Corsini *et al*., 2009 and 2010; Kim *et al*., 2011 and 2014; Khaleghi, 2015a and 2015b). For the present investigation, finer grid test is not conducted considering the total number of mesh cells is already one order of magnitude larger than those applied in the previous numerical investigations.

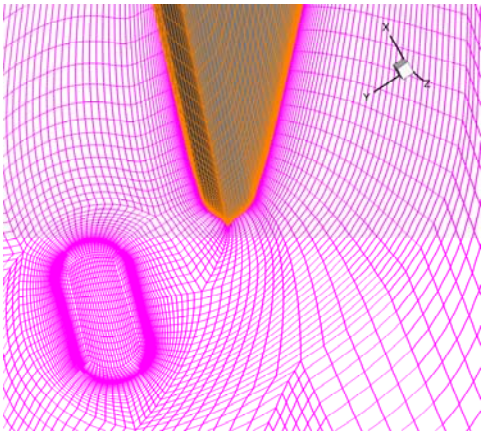

(a) Original fan

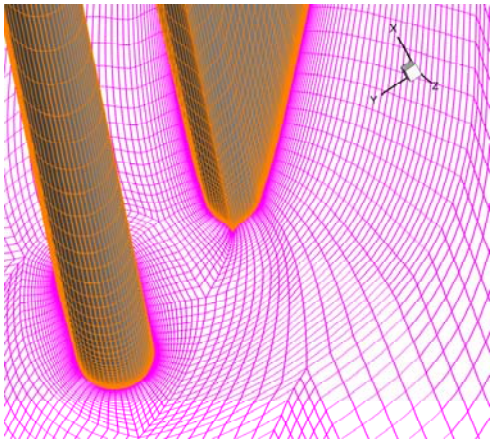

(b) Fan equipped with microplates

Fig. 6. Zoom of the grid near the leading edge at the root section.

4. RESULTS AND DISCUSSION

The fan performance is commonly presented by means of total efficiency η and static pressure coefficient ψ versus flow coefficient φ. These nondimensional coefficients are defined as follows:

$$\eta = \frac{\Delta P_t \cdot Q}{\tau \cdot \omega} \tag{1}$$

$$\psi = \frac{2 \cdot \Delta P_s}{\rho \cdot u_c^2} \tag{2}$$

$$\varphi = \frac{u_a}{u_c} = \frac{4 \cdot Q}{\pi \cdot \left(D_c^2 - D_h^2\right) \cdot u_c} \tag{3}$$

In the above equations, ΔP_t is the mass averaged total pressure rise from fan inlet to outlet and ΔP_s is the mass averaged static-to-static pressure rise. Q, τ, ω, ρ are the volumetric flow rate, torque, angular velocity, and air density, respectively. u_a is the average axial velocity through the fan annulus. u_c is the tangential blade-tip velocity. D_c and D_h are the diameters of casing wall and hub, respectively.

4.1 Grid Independence Test

A grid sensitivity analysis for the original fan without microplates was conducted not for a particular value of mass flow rate but for a series of values covering a large range, which is reflected by the nondimensional flow coefficient. A number of simulations were run for the coarse and fine grids to achieve grid-independent solutions. Two selected parameters (efficiency and static pressure) are used to show the numerical differences from the two different densities of mesh. As shown in Fig. 7a, the graphical curve, which shows the variation of total efficiency with flow coefficient, remains almost unchanged when the grid is refined. In addition to the total efficiency, the variation of static pressure coefficient versus flow coefficient is also depicted to examine the mesh effects, which is shown in Fig. 7b. The numerical results from the two grids are very small, although the differences presented in the curves of static pressure are discernable especially at low flow rates. Further grid refinement was not conducted considering the huge computation already involved and longer calculating time needed for the evaluation. As for the fan equipped with microplates, the fine grid was adopted to accurately simulate the flow passing through the gaps between the microplates and the fan blades.

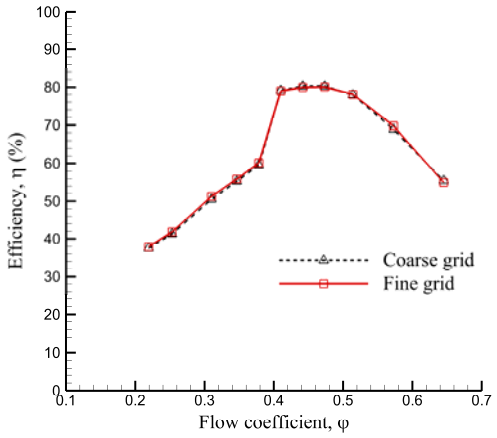

(a)

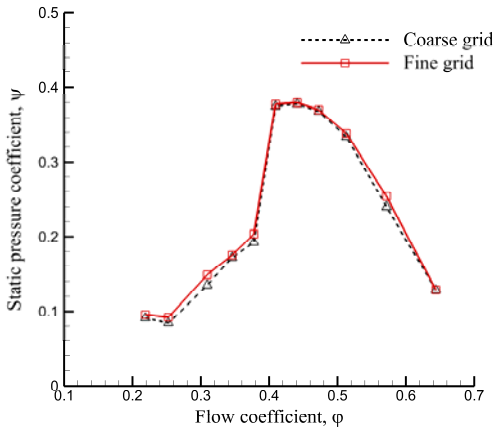

(b)

Fig. 7. Results of grid-dependency test.

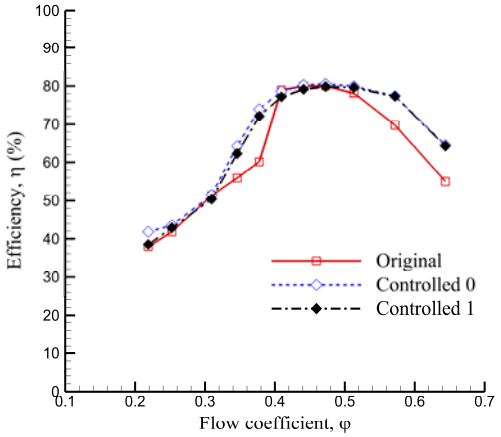

(a) Total efficiency

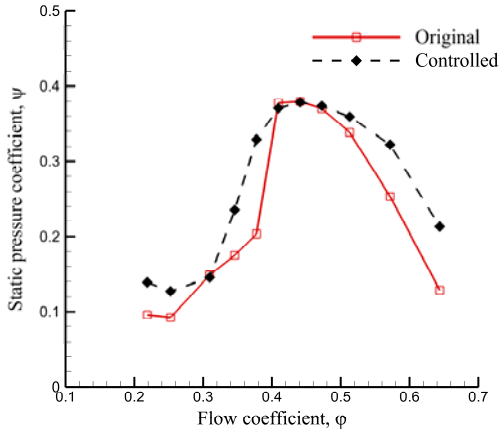

(b) Static pressure rise

Fig. 8. Comparison of characteristic curves between the original fan and the controlled fan equipped with microplates.

4.2 Overall Performance Study

Figure 8 shows the total efficiency and static pressure rise at various flow rates for the fans with and without microplates, corresponding to the line legends labeled with the names "Controlled" and "Original", respectively. As shown in Fig. 8a, the curve "Controlled 1" corresponds to the actual efficiency. The total torque on the rotor includes two parts. One part is for the fan blades and the other is for the microplates. The additional torque on the microplates should be considered. If it is subtracted from the total torque, the computed efficiency, which corresponds to the curve "Controlled 0", will be slightly higher than the actual efficiency (generally not exceeding 2%). The additional power loss due to the microplates can be ignored when the controlled fan operates at high flow rates. At the design flow coefficient (φ=0.472), the maximum efficiency of both the original and controlled fans have almost the same value, about 80%. As the flow coefficient decreases from φ=0.472 (the design point) to φ=0.409, the total efficiency (η)-flow coefficient (φ) curve tends to drop gently, which correlates with a relatively

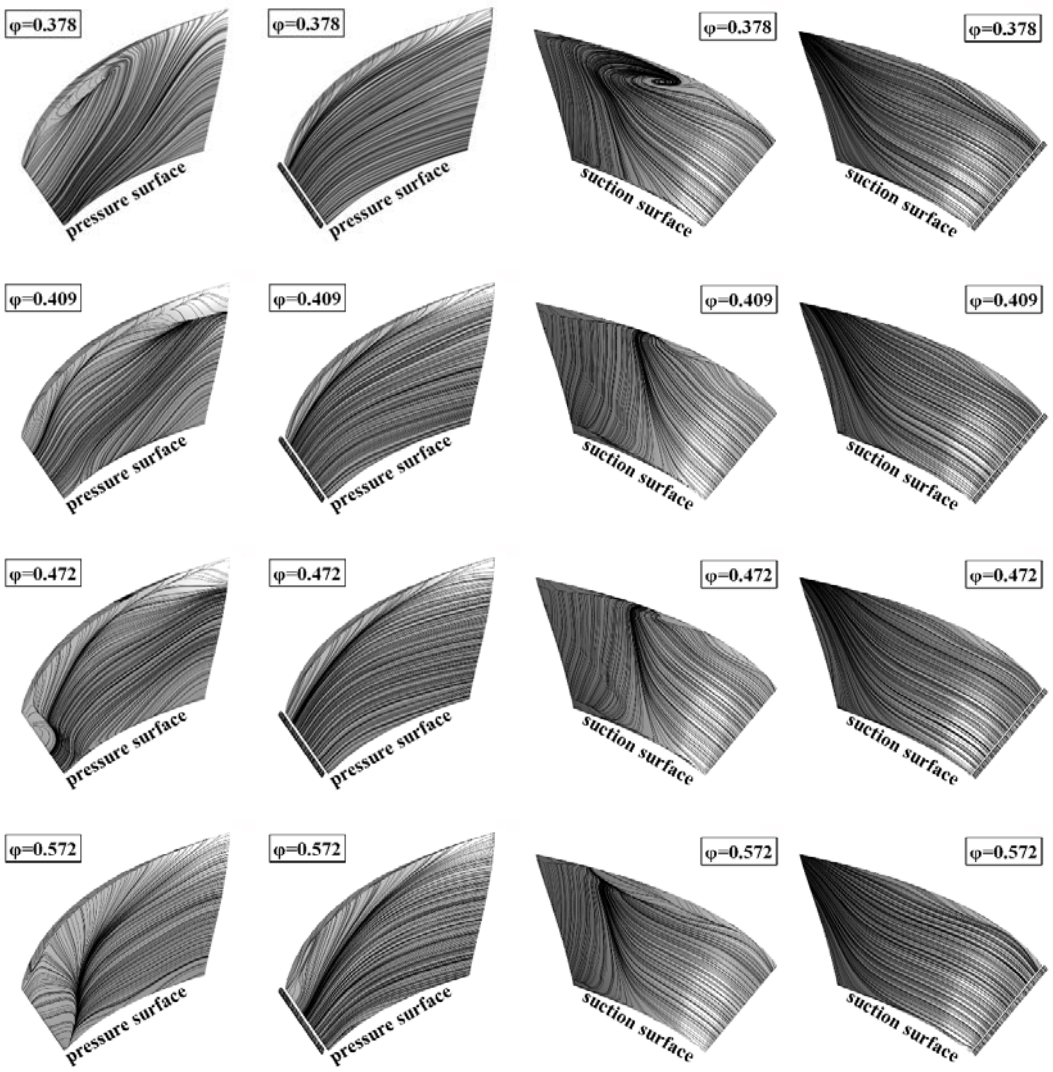

Fig. 9. Comparison of blade surface streamlines for the original and controlled fans operating at various flow rates.

mild stall. For the range of flow rates examined in this study, the total efficiency of the controlled fan has a maximum reduction at φ=0.409 but not exceeding 2%, compared with the efficiency of the original fan. As the flow coefficient further decreases, the total efficiency of the original fan starts to drop rapidly where a large part of the blade operates in deep stall. However, the total efficiency curve for the controlled fan shows a more gradual drop. In the range of φ=0.346~0.378, a significant enhancement in the efficiency is observed. When the flow coefficient φ<0.309, severe blockage of passages occurs and the microplates almost do not work. At such low flow rates, the total efficiency is not enhanced. On the other hand, when the flow coefficient increases exceeding the designed value, the total efficiency for both two fans starts to decrease. However, when compared to the original fan operating at the same flow rate, it is noted that the efficiency for the controlled fan is increased from 1.6% to 9.3% as the flow coefficient changes from 0.513 to 0.644.

The curves of static pressure coefficient versus flow coefficient are plotted in Fig. 8b. The maximum static pressure rise occurs at φ=0.441, which is slightly lower than the designed flow coefficient. In the range φ=0.409~0.472, the static pressure coefficient of the controlled fan has little change in comparison with that of the original fan. Outside this range, it is noted that the static pressure coefficient is generally increased due to the presence of microplates.

4.3 Investigation of Flow Fields

Figure 9 shows the streamlines of relative velocity on the blade surfaces at various flow rates. As for the original fan without microplates, a large recirculation region is evidently observed at φ=0.378 on the suction surface near the blade tip. At the high flow coefficient φ=0.572, massive flow separation can be distinguished on the pressure surface near the leading edge. Comparatively, as for the controlled cases, the large recirculation region is

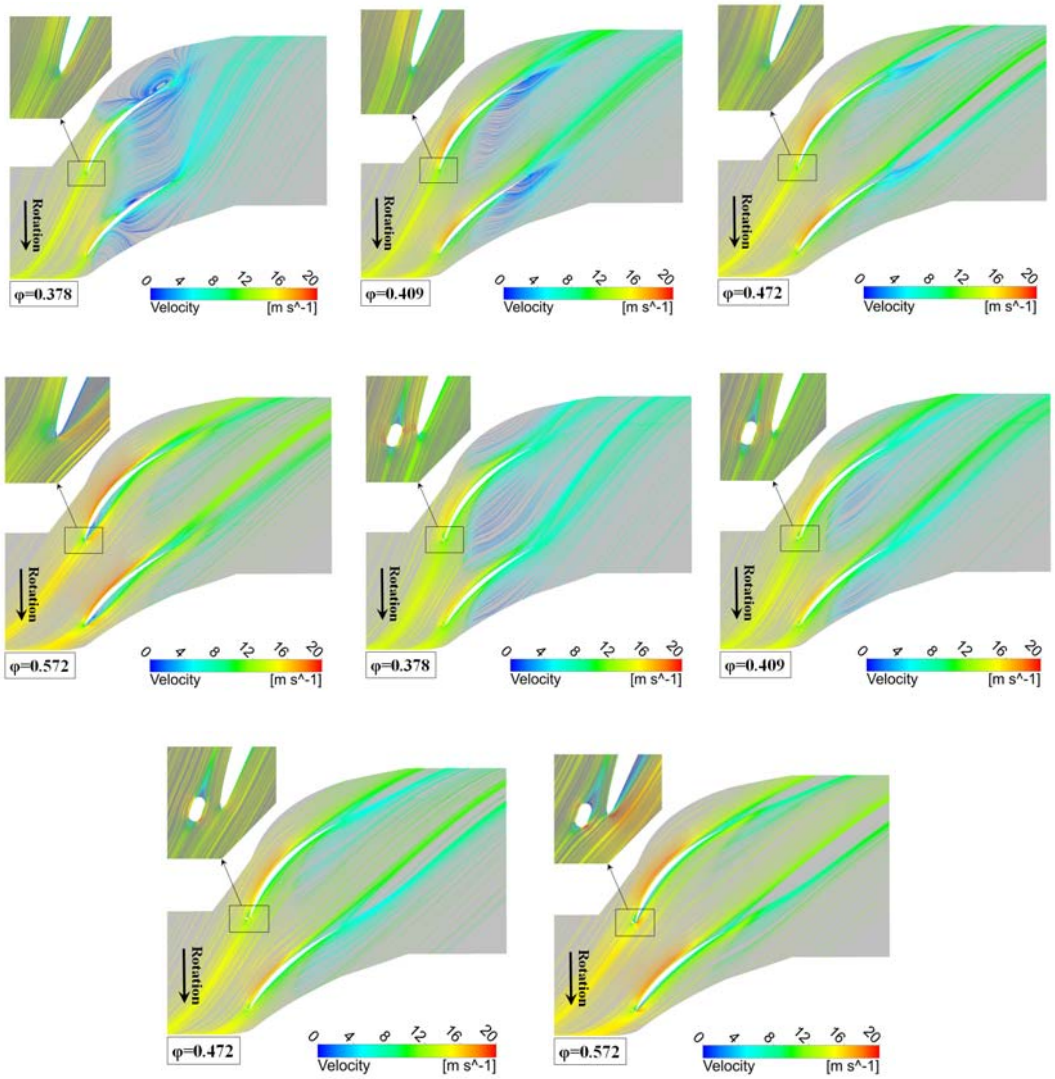

Fig. 10. Streamlines of relative velocity at 80% span for the original and controlled fans.

completely eliminated and the massive flow separation is almost fully controlled, which is responsible for the significant enhancement in the total efficiency. Additionally, from the view of streamlines on the pressure surface, one can notice that mild trailing edge separation near the blade tip occurs at φ=0.409, while shallow leading edge separation from the mid span to the tip occurs at the designed flow coefficient φ=0.472. When the microplates are placed near the blade leading edges, the flow separation at the corresponding locations disappears. Meanwhile, radial flow migration on the blade surfaces is diminished at all examined flow rates with the presence of microplates. The diminishment of radial flow migration is more pronounced on the suction surface than on the pressure surface. Radial migration not only modifies the actual geometrical features of the blade sections but also introduces additional flow loss. The effective chord length, camber and thickness distribution of the blade sections will not be consistent with the expected design states, as the migration enhances the three-dimensional effects of blade passage flow. In addition, the blade-tip flow loss is also increased as the radial flow migrates outward. It is indicated that more stable flow around the fan blades can be obtained under the control of microplates. At the vicinity of the design point, the stable flow will probably be helpful to control the noise of axial flow fans, although no enhancement in the total efficiency can be obtained with the microplates.

Figure 10 presents the streamlines of relative velocity in two passages at 80% of the blade span. At the low flow coefficient φ=0.378, large scale separation occurs near the trailing edges on the suction side of the original fan blades. The flow cells in the two adjacent passages are strongly interacted with each other and they are not rotational periodic, as the original fan operates in deep stall. Comparatively, as for the controlled fan equipped with microplates, the flow is accelerated through the two blade passages and there are no

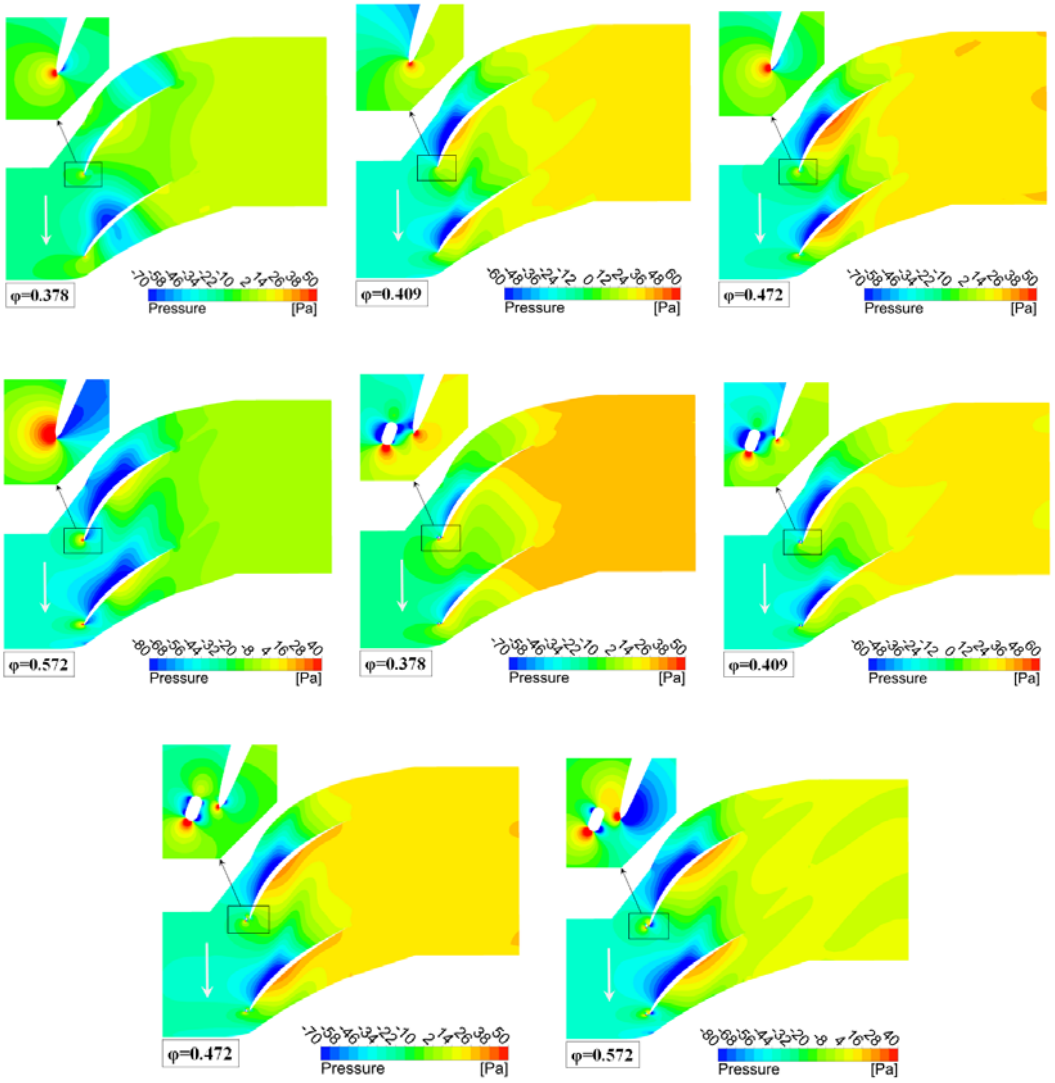

Fig. 11. Static pressure contours at 80% span for the original and controlled fans.

distinguishable separation regions. The incoming flow incidence has been adjusted by the microplates. Part of the incoming flow is redirected to the pressure side as expected. Stable flow through the controlled fan is obtained and the rotational periodicity of the flow cells for each blade passage is retained. At the high flow coefficient φ=0.572, the extent of massive leading edge separation on the pressure side is significantly reduced due to the flow guiding of microplates. Subregions of the suction surfaces near the leading edges are shielded and part of the incoming flow is squeezed to change its flow direction. Additionally, when the flow coefficient is kept at the vicinity of design point, slight improvement of the streamlines in the blade passages is observed with the presence of microplates. However, the total efficiency is slightly decreased as previously illustrated in Fig. 8 and the reason for this is because the additional energy loss caused by the incoming flow around the microplates.

Figure 11 presents the static pressure rise for the original and controlled fans at four flow coefficients. The pressure contours at 80% span are depicted for comparison purpose. It is observed that there is an overall increase in the static pressure at φ=0.378 and φ=0.572 with the presence of microplates, as the flow goes through the blade passages. This evident increase of static pressure rise is responsible for the significant enhancement in the total efficiency of the controlled fan. At the low flow coefficient φ=0.378, the pressure distributions in the two passages are not rotational periodic due to the large extent of reverse flow as in the previous analysis. The stagnation points occur on the suction surface of one blade and on the pressure surface of the other near the leading edges. When the local flow direction is adjusted by the microplates near the leading edges, the stagnation point on the suction side is shifted on the pressure side as expected. Meanwhile, good rotational periodicity of pressure distributions recovers under

the influence of microplates. On the other hand, in the vicinity of design flow coefficient (φ=0.409 and φ=0.472), static pressure levels at outlet are almost unchanged for the two fans operating at the same flow rate. However, it is observed that the static pressure on the pressure side of the fan with microplates are slightly lowered, which may be the reason that no enhancement of fan efficiency is obtained in the vicinity of design point, though the distribution of streamlines depicted on blade surface is improved.

5. CONCLUSIONS

Microplates were proposed in this study to be installed near the leading edges of blades aiming at improving the aerodynamic performance of low-speed axial flow fans. CFD simulations were performed to assess the effectiveness of this passive flow control technique in suppressing flow separation on fan blades. The performance and flow fields of the fans with and without control were compared to investigate the underlying flow control mechanisms of microplates.

At the design flow rate, microplates are unable to increase the total fan efficiency, although the flow fields can be slightly improved because of the elimination of leading edge shallow separation on the pressure surfaces from the mid span to the tip. The efficiency enhancement due to the improvement of flow fields is dissipated by the energy loss of incoming flow around the microplates. Therefore, a slight reduction in the total efficiency is observed with the presence of microplates, as the flow rate slightly decreases from the design point. However, the maximum reduction is not exceeding 2%, which is acceptable as this negative impact on fan efficiency can disappear when the fan operates at other off-design values of flow rate.

As the fans fall into a deep stall, the controlled fan can achieve a considerably higher efficiency than the original fan. On the other hand, at high flow coefficients (φ=0.513~0.644), the efficiency enhancement can be obtained from 1.6% to 9.3% as the flow rate increases beyond the design point. The reason mainly lies in the fact that flow separation on blade surfaces is effectively suppressed due to the flow guiding effects of microplates. At the low and high flow rates, comparison of surface streamlines confirms that microplates diminish the radial migration of boundary layer flow on blade surfaces especially on the suction side. In addition, at very low flow rates, the microplates almost do not work due to severe blockage occurs in the blade passages.

To sum up, as the flow rate changes, the variation of total efficiency for the controlled fan behaves more gently than the original fan without control. Fan stall can be effectively alleviated under the influence of microplates, which is favorable when the fan operates at off-design conditions. More stable flow fields and the improved overall performance can be obtained under this passive flow control.

Performance improvement of the fan equipped with straight microplates is explicitly presented by comparisons based on numerical results between controlled and uncontrolled cases. Microplates with some degrees of sweep or twist angle might be more appropriate for the rotor with twist blades. However, it will make the structure be more complicated and the benefits from microplates should be further confirmed by in-depth investigations. Besides, further experimental investigations will be performed to confirm the control effects of microplates. The current work can provide some guiding significance and reference value for this type of passive flow control in axial flow fans.

ACKNOWLEDGEMENTS

This work was supported by the National Natural Science Foundation of China (Grant No. 51536006) and the program of the Shanghai Science and Technology Commission (Grant No. 17060502300). The authors gratefully acknowledge this support.

REFERENCES

Azimian, A. R., R. L. Elder and A. B. McKenzie (1990). Application of recess vaned casing treatment to axial flow fans. *Journal of Turbomachinery-Transactions of the ASME 112*(1), 145-150.

Bianchi, S., A. Corsini, A. G. Sheard and C. Tortora (2013). A critical review of stall control techniques in industrial fans. *ISRN Mechanical Engineering* 1-18.

Bianchi, S., A. Corsini, L. Mazzucco, L. Monteleone and A. G. Sheard (2012). Stall inception, evolution and control in a low speed axial fan with variable pitch in motion. *Journal of Engineering for Gas Turbine and Power-Transactions of the ASME 134*(4), 042602.

Corsini, A., F. Rispoli and A. G. Sheard (2009). Aerodynamic performance of blade tip end-plates designed for low-noise operation in axial flow fans. *Journal of Fluids Engineering-Transactions of the ASME 131*(8), 081101.

Corsini, A., F. Rispoli and A. G. Sheard (2010). Shaping of tip end-plate to control leakage vortex swirl in axial flow fans. *Journal of Turbomachinery-Transactions of the ASME 132*(3), 031005.

Corsini, A., G. Delibra and A. G. Sheard (2013). On the role of leading-edge bumps in the control of stall onset in axial fan blades. *Journal of Fluids Engineering-Transactions of the ASME. 135*(8), 081104.

Corsini, A., G. Delibra, F. Rispoli, A. G. Sheard and D. Volponi (2014). Investigation on anti-stall ring aerodynamic performance in an axial flow fan. *ASME Turbo Expo 2014: Turbine Technical Conference and Exposition*,

Düsseldorf, Germany.

Hill, S. D., R. L. Elder and A. B. McKenzie (1998). Application of casing treatment to an industrial axial-flow fan. *Proceedings of the Institution of Mechanical Engineers, Part A: Journal of Power and Energy 212*(4), 225–233.

Khaleghi, H. (2015a). Stall inception and control in a transonic fan, part A: rotating stall inception. *Aerospace Science and Technology 41*, 250–258.

Khaleghi, H. (2015b). Stall inception and control in a transonic fan, part B: stall control by discrete endwall injection. *Aerosp. Sci. Technol.* 41, 151–157.

Kim, J. H., B. Ovgor, K. H. Cha and *et al.* (2014). Optimization of the aerodynamic and aeroacoustic performance of an axial-flow fan. *AIAA Journal 52*(9), 2032-2044.

Kim, J. H., J. W. Kim and K. Y. Kim (2011). Axial-flow ventilation fan design through multi-objective optimization to enhance aerodynamic performance. *Journal of Fluids Engineering-Transactions of the ASME 133*(10), 101101.

Lemire, S., H. D. Vo and M. W. Benner (2009). Performance improvement of axial compressors and fans with plasma actuation. *International Journal of Rotating Machinery* 1-13.

Louw, F. G., T. W. von Backström and S. J. van der Spuy (2014). Investigation of the flow field in the vicinity of an axial flow fan during low flow rates. *ASME Turbo Expo 2014: Turbine Technical Conference and Exposition*, Düsseldorf, Germany.

Menter, F. R. (1994). Two-equation eddy-viscosity turbulence models for engineering applications. *AIAA Journal 32*(8), 1598-1605.

Miyake, Y., T. Inaba and T. Kato (1987). Improvement of unstable characteristics of an axial flow fan by air-separator equipment. *J. Fluids Eng.* 109(1), 36□40.

Pinto, R. N., A. Afzal, L. V. D'Souza, Z. Ansari and A. D. M. Samee (2017). Computational fluid dynamics in turbomachinery: a review of state of the art. *Archives of Computational Methods in Engineering 24*(3), 467–479

Pogorelov, A., M. Meinkey and W. Schröder (2016a). Impact of periodic boundary conditions on the flow field in an axial fan. *AIAA Paper* 2016-0610.

Pogorelov, A., M. Meinkey and W. Schröder (2016b). Effects of tip-gap width on the flow field in an axial fan. *International Journal of Heat and Fluid Flow 61, Part B*, 466–481

Sheard, A. G. and A. Corsini (2011). The impact of an anti-stall stabilisation ring on industrial fan performance: implications for fan selection. *ASME 2011 Turbo Expo: Turbine Technical Conference and Exposition Vancouver*, British Columbia, Canada.

Suder, K. L., M. D. Hathaway, S. A. Thorp, A. J. Strazisar and M. B. Bright (2001). Compressor stability enhancement using discrete tip injection. *Journal of Turbomachinery-Transactions of the ASME 123*(1), 14-23.

Yamaguchi, N., M. Ogata and Y. Kato (2010). Improvement of stalling characteristics of an axial-flow fan by radial-vaned air-separators. *Journal of Turbomachinery-Transactions of the ASME 132*(2), 021015.

Zhu, X., W. Lin and Z. Du (2005). Experimental and numerical investigation of the flow field in the tip region of an axial ventilation fan. *Journal of Fluids Engineering-Transactions of the ASME 127*(2), 299-307.